www.vbripress.com/aml, DOI: 10.5185/amlett.2016.6169 Published online by the VBRI Press in 2016

Tunneling effect of photon-assisted AZO/SiOx/n-Si heterojunction device at reverse bias

H. W. Du, J. Yang, F. Xu, L. Zhao, Z. Q. Ma*

SHU-SolarE R&D Lab, Department of Physics, Shanghai University, Shanghai 200444, China

*Corresponding author. Tel: (+86) 21-6613-6912; Fax: (+86) 21-6613-6907; E-mail: zqma@shu.edu.cn

Received: 14 September 2015, Revised: 03 November 2015 and Accepted: 05 March 2016

ABSTRACT

Physical asymmetrical Metal / AZO / SiO_x / n-Si / Metal devices in semiconductor-insulator-semiconductor (A-SIS) framework were investigated for their anormaly current-voltage characteristics under light irradiation. The devices showed a normal rectifying character in dark but manifested a peculiar current-voltage feature at reverse bias under illumination. Considering the change of energy band structure at the reverse electric field, it was found that the transport of electrons was mainly dominated by the thermionic emission and quantum tunneling at low voltage. With the increase of the reverse bias, the electrons were able to tunnel through the reduced barrier of ultra-thin SiO_x layer (<1nm) and an effective triangle-like barrier of silicon. An appropriate simulation of the J-V relationship demonstrated that the photons acting as the assisted part magnified the reverse current density, and the thickness of SiO_x layer managed the amount of the reverse saturation current. Copyright © 2016 VBRI Press.

Keywords: Tunneling device; semiconductor-insulator-semiconductor structures; oxidation; photoconduction.

Introduction

The heterojunction diode of ZnO/Si being composed of one kind of TCO thin film and crystal silicon substrate is expected to be a device with the potential application in the photoelectric field, such as light-emitting diodes (LEDs) [**1, 2**], ultraviolet (UV) detectors [**3**] and photovoltaic cell (PV) [**4-8**]. However, the lattice mismatch of ZnO and Si could not be neglected for the interface state occurred to restrict the transport of carriers [**9, 10**]. In order to address this problem, an idea of interfacial passivation by silicon oxide is recommended to reduce the breeded surface state from the atomic hang bonds or absorption of impurity on silicon surface. Normally, ZnO/SiO_x/Si device was denoted as semiconductor insulator semiconductor (SIS) structure in the past [**11-13**]. Because of a high energy barrier raised from SiO_x layer in SIS device [**14, 15**], it was concluded that the main current passing through the barrier should be ascribed to be a quantum tunneling mechanism of the carrier transport while the device was working. The aluminum doped ZnO (AZO) is a typical transparent-conductive-oxide (TCO) and possesses advanced traits of high stability, low resistivity, and cost effective [**16, 17**], which is considered to be a competent material in the asymmetrical materials system (A-SIS device) acting as both a window layer and an emitter function. Originally, we have been looking for the likely photovoltaic (PV) property of the A-SIS structure with a simple metal/AZO/SiO_x/Si/metal configuration, and/or exploit its opto-electronic features in the semiconductor industry fields. However, the fact is going beyond of our objective. After we fabricated a matured device, an aberrant phenomenon was occurred, i.e., there is a gradual amplification of the reverse current with the increase of the negative bias from -1.0 to - 4.0 V, especially, the reverse current is maintained at a saturation value in the range of about - 3.5 to - 4.0 V. The unusual optoelectronic property has been observed with the reduced thickness of SiO_x buffer layer in the scope of 0.5-1.0 nm within AZO/SiO_x/Si heterojunction structure, rather than PV characteristics for the metal/AZO/SiO_x/Si/metal device. What is the mechanism by which results in the change of physical parameters on the device?

In order to make clear the observation mentioned above, we try to set up a model on the carrier transport through the barrier, and a simulation has been carried out for the interpretation of the optoelectronic conductivity with the quantum tunneling solution as a significant understanding.

Experimental

In this work, three ultra-thin silicon oxide layers with the different thicknesses were fabricated on the textured *n*-Si (100) wafers (carrier density: 2.0×10^{-15} cm^{-3}) by a rapid thermal oxidation process at 800 °C for 1.0, 2.0 and 3.0 min, respectively. Then, about 300 nm AZO layer (carrier density: 4.2×10^{-20} cm^{-3}) was direct deposited by direct current (d.c) magnetron sputtering technique on the oxidized Si wafer to assemble the heart of A-SIS device. At last, Al/Ni and Mg/Al metal alloy were deposited on the front and rear of the samples by vacuum thermal evaporation, respectively, by which the Ohmic contacted front grids and back electrodes were successfully formed. The current-voltage characteristics of the A-SIS device were measured at room temperature and the mechanism of carriers transport at reverse bias voltage both under dark and illumination conditions were discussed.

Results and discussion

In the experiment, the current-voltage (*I-V*) characteristics of A-SIS devices in dark and illumination conditions were examined. The polarity of the applied direct current for the I-V measurement was assigned to positive at the AZO side and negative at the n-Si side. At dark condition, the I-V characteristic of A-SIS device with 1.0 min oxidation time (OT) for SiO_x layer is presented as squared hollow dots line in **Fig. 1**, which exhibits good rectifying character with rectification ratio of 1230 at ±2.0 V. While the device was placed in illumination of halogen lamp with 30mW/cm^2, the I-V characteristic was transformed to be an uncommon curve rather than an expectant photovoltaic character, shown as the red circle dots line in **Fig. 1**. At forward bias, the I-V characteristic still obeys the rule of Shockley ideal diode equation with an ideal factor of 3.88, i.e., the current has an exponential increase, and the current density is in the range of several tens of mA·cm^{-2}. However, at reverse bias, the current does not keep saturation until the bias approaching a higher value of -3.0 V, and there is a threshold voltage at -1.0 V. The same phenomenon appeared in the other two devices with the same solid structure while the different silicon oxidation times adding to 2.0 and 3.0 min were performed, respectively. The results were showed as blue and green triangle dotted line in **Fig. 1**. With the increase of the oxidation time, the photon-excited correlative current density was dramatically decreased from 25.7 to 8.1 mA·cm^{-2}. The fact has been verified and the novelty has rarely been observed for the device with the same kind architecture and materials.

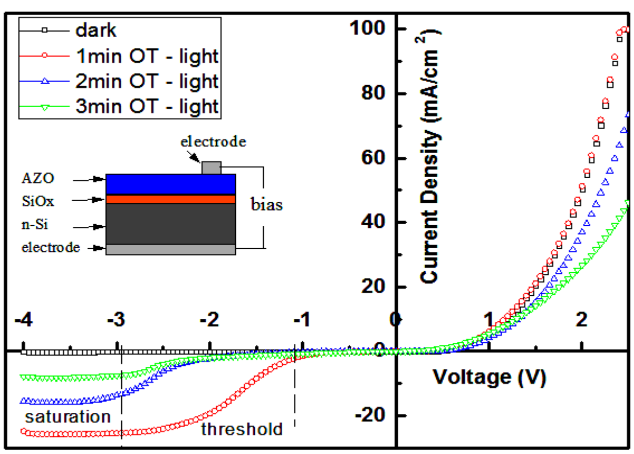

Fig. 1. Current density-voltage characteristics of metal/AZO/SiO_x/n-Si/metal devices with the different thicknesses of SiOx, fabricated by RTO technique under dark and illumination; the different thicknesses of SiO_x layers are determined by the oxidation time (OT).

To well understand the variation of the current with the reverse bias for these devices under illumination, the charge occurrence, transport and collection in the heterojunction semiconductor device has been taken into account. It is well known that the property of the semiconductor devices closely related to the energy band structure in the intermediate region. In our investigation of the A-SIS device, the electronic affinity of ZnO:Al and n-Si are 4.35 and 4.05 eV, respectively. Because of ZnO:Al with very high electron concentration of 4.24 × 10^{20}cm^{-3}, the Fermi level of ZnO:Al closely lay on the bottom of conduction band [**18**], which results in both ZnO:Al and n-Si almost have a little difference of work function. **Fig. 2**(**a**) illustrates the energy band structure of the heterojunction semiconductor materials at the equilibrium state. The physical factors influencing the transport of carriers are shown by ΔE_c, the energy band discontinuous part, the potential barrier and the interface states. **Fig. 2** (**b**) and (**c**) show the variation of the energy band of AZO/SiO_x/n-Si at low and high reverse bias, respectively, in which the difference in the conduction band edges is ΔE_c= 0.3 eV. At low reverse bias, the transport of electrons from AZO to Si is believed to be mainly dominated by the thermionic emission and then tunneling and/or recombination processes, because the tunneling cannot occur at nearly the same energy level based on the WKB approximation [**19**]. In general, with the increase of the reverse bias, the energy band in Si side begin to bend to an appropriate level to enable the electron tunneling through the high barrier of ultra-thin SiO_x layer and triangle barrier. Here the interface states and the inductive space charge field may act as a "tunneling-recombination bridge" for the detected current density. The same behavior of quantum tunneling was also observed in another similar device system [**20**].

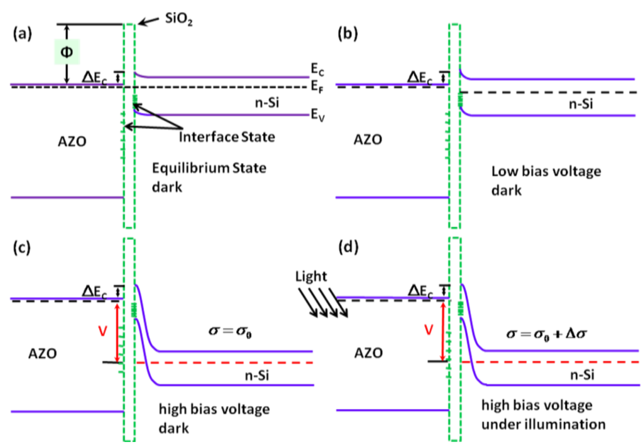

Fig. 2.The energy band diagram of AZO/SiO_x/n-Si junction at (a) thermal equilibrium; (b) at low reverse bias; (c) at high reverse bias; (d) at high reverse bias and under illumination.

Under dark condition, the reverse saturation current density is about 1.1×10^{-4} mA·cm^{-2} , as shown in **Fig. 1**, which indicates that the amount of tunneling and thermionic emission current are very low. On the contrary, the reverse current density increases to 25.7 mA/cm^2 under light irradiation, which may predict an additional conductance associated with the photon injection. The probability of the increased current at a higher adverse bias is correlated to the character of the device structure and the formation of energy barrier between the AZO film and n-Si. The carrier transport mechanism is significantly needed to elucidate the observation at the moment.

Based on the above analysis, a complex function of current density (J) on reverse bias (V) is here proposed to explain the current-voltage characteristics at reverse bias as follows:

$$J = -KA(\sigma)\begin{cases} T(d_{ox})E(V) & \text{small bias} \\ T(S) & \text{large bias} \end{cases} \qquad (1)$$

where, $A(\sigma)$ is photon-assisted part, $T(S)$ is an effective tunneling part of the alterable barrier shape, $T(d_{ox})$ is WKB-like tunneling part of SiOx barrier, $E(V)$ is thermionic emission part, and K is a materials correlated constant. The total reverse current density and the specific expressions from the different contributions have been derived as:

$$\ln(-J)=\ln KA(\sigma)-\alpha_1\sqrt{\Phi}d_{ox} - \begin{cases} \dfrac{n_s V'}{k_B T}+9.6 & (-1.2V<V'<-0.3V) \\ \dfrac{\alpha_2}{2\sqrt{C}}\left[\sqrt{\left|\Delta E_c \cdot V'\right|}-(V'+\Delta E_c)\ln\dfrac{\sqrt{|V'|}-\sqrt{\Delta E_c}}{\sqrt{|V'+\Delta E_c|}}\right] & (V'<-3V) \end{cases} \quad (2)$$

where,

$$A(\sigma)=\frac{k_B T}{qL_n}(\sigma_0+\Delta\sigma);$$

$$\alpha_1=2\sqrt{\frac{2qm_1^*}{\hbar}};\alpha_2=2\sqrt{\frac{2qm_2^*}{\hbar}}$$

$$C=\frac{qN_D}{2\varepsilon_r\varepsilon_0}$$

where, σ_0 and $\Delta\sigma$ are dark and photo-conductance increment, respectively; Φ is the barrier height of SiO_x; d_{ox} is the reduction thickness of SiO_x; m_1^* and m_2^* are the effective mass of electron in the SiO_x layer and bulk Si, respectively; n_s is the ideal factor defined by H.C. Card and E.H. Rhoderick [**21**]; *V'* is partial voltage of Si side which generally equal to total bias (V); N_D is the dopant concentration of silicon substrate; L_n is effective diffusion length of electron; q is effective charge; $\hbar$ is Plank constant; ε_r and ε_o are relative and vacuum dielectric constant of silicon, respectively; k_B is Boltzmann constant.

Table. 1. Specific parameters of A-SIS device for simulation.

Parameter	Values	Parameter	Values
k_B	1.4×10^{-23} J/K	Φ	2.2 eV
T	300 K	$\hbar$	1.1×10^{-34} J·s
q	1.6×10^{-19} c	N_D	2.0×10^{21} /cm^3
L_n	1.0×10^{-4} m	ε_r	11.9
σ_0	28.0 S/m	ε_0	8.9×10^{-12} F/m
$\Delta\sigma$	6.2×10^3S/m	m	0.49
m_1*	9.1×10^{-31} kg	n_s	0.14
m_2*	9.1×10^{-31} kg		

The values of all above parameters designed to the device are listed in **Table 1**. The natural logarithm of the current density in eq.(2) is easily separated into photon-assisted part, tunneling part through oxide layer combined with thermionic emission and tunneling part through barrier of oxide layer and Si, respectively. The larger difference of the current density in dark and light illumination conditions are dominated by the first term in eq. (2). The photon-assisted part is strongly dependent on the conductance of silicon substrate which would be bigger after absorbing photon's energy. The corresponding energy band structure is illustrated as in **Fig. 2**(**d**), where the carriers should be driven by both electrical and optical fields at the same time.

The measured data and the simulations of the current density at reverse bias of the device with the structure of metal/AZO/SiO_x/n-Si/metal for an oxidation time of 1.0 min are manifested in **Fig. 3**.

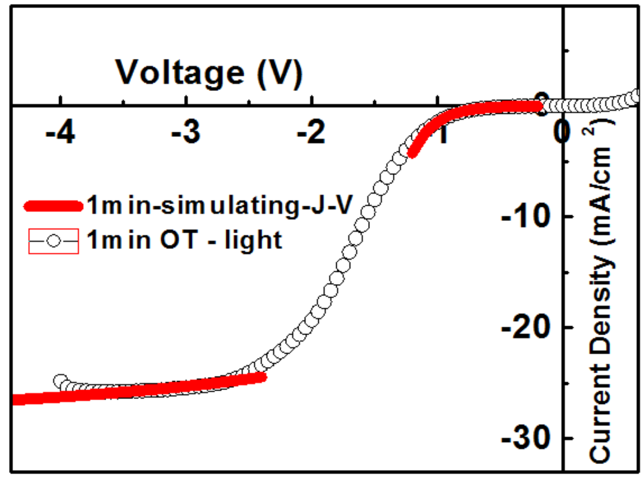

Fig. 3. The simulation and experiment results of current density at reverse bias on the Metal/AZO/SiO_x/n-Si/Metal device with 1.0 min oxidation time under illumination.

At the regions of -1.2 V < V' < -0.3 V and V' < -3.0 V, the numerical calculation of the threshold are in good agreement with the experimental observation, which demonstrates that the electron transport is controlled from partially tunneling-recombination and thermionic emission to total tunneling at the low reverse bias turning to the saturation section of high bias, respectively. In **Fig. 1**, the difference of the three samples with the different saturation current at reverse bias is tentatively interpreted by the tunneling fraction dependent on the variation of the silicon oxide layer in the eq. (2), which results from the different thicknesses of d_{ox}. The performance of the Metal/AZO/SiO_x/n-Si/Metal device at reverse bias under illumination indicates a potential application in the light-sensitive detector.

Conclusion

In summary, the physical asymmetrical optoelectronic devices of Metal/AZO/SiO_x/Si/Metal with the semiconductor-insulator-semiconductor (A-SIS) framework and the different thicknesses of SiO_x layers have been successfully fabricated by the combination RTO with dc-magnetron sputtering deposition methods. The device manifested a good rectifying character with the rectification ratio of 1230 at ±2.0 V under dark. However, the exceptional current-voltage characteristics under illumination demonstrated an attractive current amplifying feature when the reverse bias was over -2.5 V. The numerical simulation based on the transport model of carrier tunneling through a narrow barrier indicated that the transport of electrons from AZO to Si is dominated by both thermionic emission and tunneling at low reverse bias, while the electrons are able to tunnel through an effective triangle barrier of ultra-thin SiO_x layer at high reverse bias,. In the meantime, the photons absorbed by Si substrate could magnify the reverse current, which was oxide layer thickness dependent relationship.

This work was partly supported by the National Natural Science Foundation (No. 61274067 and 60876045) of China, Shanghai Leading Basic Research Project (No. 09JC1405900), and R&D Foundation of SHU-SOENs PV Joint Lab (No. SS- E0700601). This appreciation was also given to Instrumental Analysis & Research Center of Shanghai University for their help in microstructure measurements of the samples. One of authors (H.W.Du) gives his grateful to Dr. Shen Ling, Gao Ming, Li Yong, Ding Hu, and Chen Shumin for their help in experiments.

Reference

1. Ye,Z. Z.; Lu,J.G.; Zhang,Y. Z.; Zeng, Y. J.; Chen, L. L.; Zhuge, F.; Yuan, G. D.; He, H. P.; Zhu, L. P.; Huang, J. Y.; Zhao, B. H. *Appl. Phys. Lett.* **2007**, *91*, 113503.
2. Tan, S. T.; Sun, X.W.; Zhao, J. L.; Iwan, S.; Cen, Z. H.; Chen, T. P.; Ye, J. D.; Lo, G. Q.; Kwong, D. L.; Teo, K. L. *Appl. Phys. Lett.* **2008**, *93*, 013506.
3. Kang, H.; Park, J.; Choi, T.; Jung, H.; Lee, K. H. *Appl. Phys. Lett.* **2012**, *100*, 041117
4. Wenas, W.W.; Riyadi, S. *Solar Energy Materials & Solar Cells* **2006**, *90*, 3261.
5. Shen, L.; Ma, Z.Q.; Shen, C.; Li, F.; He, B.; Xu, F. *Superlattices and Microstrctures* **2010**, *48*, 426.
6. Pradhan, A. K.; Hooloway, T.; Mundle, R.; Dondapati, H.; Bahoura, M. *Appl. Phys. Lett.* **2012**, *100*, 061127.
7. Wei-Ying, Z.; Sheng, Z.; Li-Jie, S.; Zhu-xi, F. *Chin. Phys. Lett.* **2008**, *25*, 1829.
8. Jing-Jing, M.; Ke-xin, J.; Bing-cheng, L.; Fei, F.; Hui, X.; Chao-chao, Z.; Chang-le, C. *Chin. Phys. Lett.* **2010**, *27*, 10.
9. Shen, L.; Du, H.W.; Ding, H.; Tang, J.; Ma, Z.Q. *Materials Science in Semiconductor Processing* **2010**, *13*, 339.
10. Huan, L.; Ci-hui, L.; Bi-xia, L.; Zhu-Xi, F. *Chin. Phys. Lett.* **2005**, *22*,185.
11. Shewchun, J.; Burk, D.; Singh, R.; Spitzer, M.; Dubow, J. *J. Appl. Phys.*, **1979**, *50*, 6524.
12. Spitzer, M.; Shewchun, J.; Burk, D. *J. Appl. Phys.*, **1980**, *51*, 6399
13. Ghosh, A. K.; Fishman, C.; Feng, T. *J. Appl. Phys.*, **1978**,*49*, 3490.
14. Fulton, C.C.; Lucovsky, G.; Nemanich, R.J. *J. Appl. Phys.* **2006**, *99*, 063708.
15. Bersch, E.; Rangan, S.; Bartynski, R. A. *Phys. Rev. B* **2008**, *78*, 085114.
16. Kim, J.H.; Ahn, B.D.; Lee, C.H.; Jeon, K.A. *J. Appl. Phys.* **2006**, *100*, 113515.
17. Lin, Qing-geng, Xiao-yong, G.; Jin-hua,G.; Yong-sheng, C.; Shi-e, Y.; Jing-xiao, L. *Chin. Phys. Lett.* **2008**, *25*, 4223.
18. Suchea, M.; Christoulakis, S.; Katsarakis, N.; Kitsopoulos, T.; Kiriakidis, G. *Thin Solid Films* **2007**, *515*, 6562.
19. Fromhold Jr., A. T. *Quantum Mechanics for Applied Physics and Engineering, Dover, New York* **1981**.
20. Cheknane, A. *J. Phys. D: Appl. Phys.* **2009**, *42*, 115302.
21. Card, H. C.; Rhoderick E.H. *J. Phys. D: Appl. Phys.* **1971**, *4*, 1602.